Exchange effects and second-order Born corrections in laser-assisted (e, $2e$) collisions with helium atoms

I. Ajana, A. Makhoute, D. Khalil, and S. Chaddou
UFR de Physique du Rayonnement et des Interactions Laser-Matière, Faculté des Sciences, Université Moulay Ismail, B.P. 11201, Zitoune, Meknès, Morocco
(Received 7 January 2015; published 17 April 2015)

The triple differential cross section for laser-assisted ionization of a helium target by slow electrons is analyzed within the framework of the second Born approximation. We evaluate the S-matrix elements using Volkov and Coulomb-Volkov wave functions for describing the continuum states of the scattered and the ejected electrons, respectively. The required scattering amplitudes are performed by expanding the atomic wave functions onto a complex-scaled Sturmian basis, which allows us to exactly take into account the contribution of the continuous spectrum to the dressing of the atomic states. Our results have been improved by taking into account exchange effects. Furthermore, the second-order Born correction is seen to be important and significantly affects the magnitudes of the binary and recoil peaks.

DOI: 10.1103/PhysRevA.91.043411 PACS number(s): 34.50.Rk, 34.80.Dp, 34.50.Fa

I. INTRODUCTION

Electron-impact ionization of atoms is a fundamental process which is relevant to understand and interpret a wide range of scientific phenomena and technological applications, including plasma physics [1], planetary atmospheres [2], and radiation interactions with living tissue [3]. The study of such processes provides important information about target structure, target wave function, and collision dynamics. Since the pioneering (e, $2e$) experiment carried out by Ehrhardt *et al.* [4], many (e, $2e$) coincidence experiments were performed for various atomic targets and for a wide range of kinematic parameters [5–10]. Meanwhile, theoretical investigations have been performed to calculate the triple differential cross section (TDCS) using different models [9–16]. In the past few years, there has been particular interest for the study of (e, $2e$) processes in the low-incident-energy regime in coplanar symmetric geometry [17–20]. A number of theoretical calculations [21–29] exist in the literature for the laser-assisted (e, $2e$) process of hydrogen and helium atoms, prior to the first realization of the kinematically complete experiment of Höhr *et al.* [30] for the laser-assisted single ionization of a helium atom.

The first theoretical treatment in which all the characteristic features of the experiments of Ehrhardt *et al.* were reproduced was a second Born calculation of the (e, $2e$) triple differential cross sections performed by Byron *et al.* [31] in atomic hydrogen. Pathak and Srivastava [32] used the second Born approximation for the ionization of atomic hydrogen and compared their results to the first (e, $2e$) experiments of Weigold *et al.* [33]. Then they also made calculations for the ionization of helium by using the closure approximation and compared their results to those of Ehrhardt *et al.* [34]. Byron *et al.* [35] also calculated TDCSs for the ionization of helium by using the closure approximation and found results which disagreed with those of Pathak and Srivastava [32]. Later on, Byron *et al.* [36] applied the second Born approximation by using very few discrete states as intermediate states and by taking into account the closure approximation and adding the contribution of the third Born approximation calculated with the Glauber approximation. It was found that the second Born calculation plays a crucial role in understanding the (e, $2e$) process. The comparison between experiment and theory showed that second-order effects are essential in explaining the angular positions, shapes, and magnitudes of both the binary and recoil peaks. Recently, Zheng *et al.* studied laser-assisted electron-impact [37] and positron-impact [38] ionization of atomic hydrogen in the second Born approximation. They found that the second-order corrections are significant and that the second Born results for electrons and positrons show some obvious discrepancies.

The Born approximation has been most widely used to calculate ionization cross sections. This model is flexible in analytical and numerical calculations and remains a preferable model to investigate the collision processes. At sufficiently high energies it is generally believed that the first Born approximation can be used to describe the direct ionization process. It is therefore obviously necessary to extend the Born approximation by treating the projectile-target interaction up to second-order Born amplitude in the range of the low-energy regime. In this paper, we investigate the application of the second Born approximation (SBA) for the laser-assisted single ionization of a helium atom by low-energy electrons. This formalism is improved by the consideration of the exchange effect between the free outgoing electrons. Most work on the laser-assisted (e, $2e$) reactions employed the first Born approximation (FBA) [25,39–41], due to the difficulty of the numerical calculation of the second Born term. In fact, the second Born approximation needs a difficult triple numerical integration [42] and often many authors find some controversial results. The present work extends our previous study [43] on laser-assisted (e, $2e$) collisions of atomic hydrogen using a second Born treatment which includes the double interaction between the incoming electron and the target.

The remainder of this paper is presented in four sections. Section II describes the theoretical treatment of the ionization process. Our second- and first-order Born results are presented and discussed in Sec. III. Finally, Sec. IV draws conclusions from this investigation. Atomic units are used throughout unless otherwise stated.

II. THEORY

During a laser-assisted electron-impact ionization process, ℓ photons may be exchanged with the laser field. Schematically, the laser-assisted $(e, 2e)$ reaction of a helium atom can be written as

$$e^-(\boldsymbol{k}_i) + \mathrm{He}(1^1S) + \ell\omega \longrightarrow \mathrm{He}^+ + e^-(\boldsymbol{k}_a) + e^-(\boldsymbol{k}_b), \quad (1)$$

where positive integer values of ℓ correspond to the photon absorption, negative integer values to photon emission, and $\ell = 0$ to the $(e, 2e)$ process in a laser background with no net transfer of photons; ω refers to the laser frequency and $\boldsymbol{k}_i$, $\boldsymbol{k}_a$, and $\boldsymbol{k}_b$ are, respectively, the momenta of the incident, scattered, and ejected electrons. We assume that the laser field is treated classically as a single-mode, spatially homogenous, monochromatic, linearly polarized electric field

$$\boldsymbol{\mathcal{E}}(t) = \boldsymbol{\mathcal{E}}_0 \sin(\omega t + \varphi). \quad (2)$$

The corresponding vector potential is $\boldsymbol{A}(t) = \boldsymbol{A}_0 \cos(\omega t + \varphi)$ with $\boldsymbol{A}_0 = c\,\boldsymbol{\mathcal{E}}_0/\omega$ and φ is the initial phase.

The energy conservation equation corresponding to the laser-assisted $(e, 2e)$ reaction of Eq. (1) reads

$$E_{k_i} + E_0^{\mathrm{He}} + \ell\omega = E_0^{\mathrm{He}^+} + E_{k_a} + E_{k_b}, \quad (3)$$

where $E_0^{\mathrm{He}} = -2.90372$ a.u. is the ground-state energy of helium and $E_0^{\mathrm{He}^+} = -2$ a.u. the ground-state energy of He^+. $E_{k_i} = k_i^2/2$, $E_{k_a} = k_a^2/2$, and $E_{k_b} = k_b^2/2$ represent the kinetic energies of the incident, scattered, and ejected electrons, respectively.

As in our previous work on atomic hydrogen [43], we carry out a second Born treatment of reaction (1). We are aware of the fact that higher terms of the Born series (in particular the second Born term) play a significant role in obtaining accurate values of TDCSs for laser-assisted $(e, 2e)$ collisions at low incident energies. The prior form of the scattering matrix element for the process (1) in the first Born approximation is

$$S_{\mathrm{ion}}^{B_1} = -i \int_{-\infty}^{+\infty} dt \langle \psi_f | V_d | \psi_i \rangle, \quad (4)$$

where V_d is the electron-atom interaction potential given by

$$V_d = -\frac{2}{r_0} + \frac{1}{r_{01}} + \frac{1}{r_{02}}. \quad (5)$$

In this equation $\boldsymbol{r}_0$ denotes the coordinate of the incident (and scattered) electron, $\boldsymbol{r}_1$ and $\boldsymbol{r}_2$ are the coordinates of the target electrons, $r_{01} = |\boldsymbol{r}_0 - \boldsymbol{r}_1|$, and $r_{02} = |\boldsymbol{r}_0 - \boldsymbol{r}_2|$. The wave function ψ_i is the asymptotic initial-state wave function and ψ_f is the final-state wave function satisfying the incoming wave boundary condition. It is evident from Eq. (4) that the perturbation V_d vanishes asymptotically for $r_0 \to \infty$.

In the present model the projectile-laser interaction is treated to all orders while the laser-target interaction is considered in the framework of the first-order time-dependent perturbation theory. The initial channel asymptotic wave function ψ_i is chosen as $\psi_i(\boldsymbol{r}_0,\boldsymbol{r}_1,\boldsymbol{r}_2,t) = \chi_{k_i}(\boldsymbol{r}_0,t)\phi_0(\boldsymbol{r}_1,\boldsymbol{r}_2,t)$, where $\chi_{k_i}(\boldsymbol{r}_0,t)$ denotes the plane-wave Volkov solution for the laser dressed incident electron with momentum k_i. It is given by expression of the form [44]

$$\chi_k(\boldsymbol{r}_0,t) = (2\pi)^{-\frac{3}{2}} \exp[i(\boldsymbol{k}\cdot\boldsymbol{r}_0 - \boldsymbol{k}\cdot\boldsymbol{\alpha}_0 \sin(\omega t) - E_k t)], \quad (6)$$

where $\boldsymbol{k}$ denotes the electron wave vector, $E_k = k^2/2$ is its kinetic energy, and $\boldsymbol{\alpha}_0 = \frac{\boldsymbol{\mathcal{E}}_0}{\omega^2}$ is the amplitude associated with the classical quiver motion of the electron in the laser field. The Volkov wave function of Eq. (6) is normalized to a δ function.

The wave function $\phi_0(\boldsymbol{r}_1,\boldsymbol{r}_2,t)$ represents the dressed wave function of the ground-state helium atom [45]:

$$\phi_0(\boldsymbol{r}_1,\boldsymbol{r}_2,t) = e^{-i\boldsymbol{a}\cdot\boldsymbol{R}} e^{-iE_0^{\mathrm{He}}t}\Bigg[\psi_0(\boldsymbol{r}_1,\boldsymbol{r}_2) + \frac{i}{2}\sum_j \left(\frac{e^{i\omega t}}{E_j - E_0^{\mathrm{He}} + \omega} - \frac{e^{-i\omega t}}{E_j - E_0^{\mathrm{He}} - \omega}\right) \times M_{j0}\,\psi_j(\boldsymbol{r}_1,\boldsymbol{r}_2)\Bigg], \quad (7)$$

where $\boldsymbol{a}(t) = \boldsymbol{A}(t)/c$ and $\mathbf{R} = \boldsymbol{r}_1 + \boldsymbol{r}_2$, ψ_j is the unperturbed wave function of the helium atom of energy E_j, and $M_{j0} = \boldsymbol{\mathcal{E}}_0 \cdot \langle \psi_j | \boldsymbol{R} | \psi_0 \rangle$ is a dipole-coupling matrix element. The factor $e^{-i\boldsymbol{a}\cdot\boldsymbol{R}}$ ensures the gauge consistency between the Volkov wave function of Eq. (6) and the dressed target wave function of Eq. (7).

The helium ground-state wave function ψ_0 which we used in Eq. (7) is that of Byron and Joachain [46]. It is an analytical fit to a Hartree-Fock wave function given by

$$\psi_0(\boldsymbol{r}_1,\boldsymbol{r}_2) = \phi_0^{\mathrm{He}}(\boldsymbol{r}_1)\phi_0^{\mathrm{He}}(\boldsymbol{r}_2), \quad (8)$$

where

$$\phi_0^{\mathrm{He}}(\boldsymbol{r}) = \frac{1}{\sqrt{4\pi}}(Ae^{-\alpha r} + Be^{-\beta r}), \quad (9)$$

with $A = 2.60505$, $B = 2.08144$, $\alpha = 1.41$, and $\beta = 2.61$.

The final-state wave function ψ_f is approximated as $\psi_f(\boldsymbol{r}_0,\boldsymbol{r}_1,\boldsymbol{r}_2,t) = \chi_{k_a}(\boldsymbol{r}_0,t)\phi_{k_b}(\boldsymbol{r}_1,\boldsymbol{r}_2,t)$, where $\chi_{k_a}(\boldsymbol{r}_0,t)$ refers to the scattered electron wave function in the final channel, which corresponds to the Volkov wave function given by Eq. (6). $\phi_{k_b}(\boldsymbol{r}_1,\boldsymbol{r}_2,t)$ denotes the dressed continuum wave function representing the state of an ejected electron of asymptotic momentum $\boldsymbol{k}_b$ moving in the combined field of the residual $\mathrm{He}^+(1s)$ ion and the external laser field. It is given by expression of the form [25]

$$\phi_{k_b}(\boldsymbol{r}_1,\boldsymbol{r}_2,t) = e^{-iE_{k_b}t} e^{-iE_0^{\mathrm{He}^+}t} e^{-i\boldsymbol{a}\cdot\boldsymbol{R}} e^{-i\boldsymbol{k}_b\cdot\boldsymbol{\alpha}_0\sin(\omega t)}\Bigg[\psi_{k_b}^{(-)}(\boldsymbol{r}_1,\boldsymbol{r}_2)(1 + i\boldsymbol{k}_b\cdot\boldsymbol{\alpha}_0\sin(\omega t)) + \frac{i}{2}\sum_j \left(\frac{e^{i\omega t}}{E_j - E_0^{\mathrm{He}^+} - E_{k_b} + \omega} - \frac{e^{-i\omega t}}{E_j - E_0^{\mathrm{He}^+} - E_{k_b} - \omega}\right) M_{jk_b}\psi_j(\boldsymbol{r}_1,\boldsymbol{r}_2)\Bigg], \quad (10)$$

where

$$\psi_{k_b}^{(-)}(\boldsymbol{r}_1,\boldsymbol{r}_2)=\frac{1}{\sqrt{2}}\left[\phi_0^{\mathrm{He}^+}(\boldsymbol{r}_1)\phi_{c,k_b}^{(-)}(\boldsymbol{r}_2)+\phi_0^{\mathrm{He}^+}(\boldsymbol{r}_2)\phi_{c,k_b}^{(-)}(\boldsymbol{r}_1)\right]. \tag{11}$$

Here $\phi_0^{\mathrm{He}^+}(\boldsymbol{r})=\sqrt{8\pi}\exp(-2r)$ is the $\mathrm{He}^+(1s)$ wave function, while

$$\phi_{c,k_b}^{(-)}(\boldsymbol{r})=\psi_{c,\,k_b}^{(-)}(\boldsymbol{r})-\left\langle\phi_0^{\mathrm{He}}(\boldsymbol{r})\middle|\psi_{c,\,k_b}^{(-)}(\boldsymbol{r})\right\rangle\phi_0^{\mathrm{He}}(\boldsymbol{r}) \tag{12}$$

is a modified continuum Coulomb wave function with incoming spherical wave behavior, orthogonalized to the ground-state helium orbital ϕ_0^{He}. In Eq. (12)

$$\psi_{c,\,k_b}^{(-)}(\boldsymbol{r})=(2\pi)^{-3/2}\,e^{\pi/2k_b}\,\Gamma\left(1+\frac{i}{k_b}\right)\times{}_1F_1\left[-\frac{i}{k_b},1,-(ik_br+\boldsymbol{k}_b\cdot\boldsymbol{r})\right] \tag{13}$$

is a Coulomb wave function with incoming spherical wave behavior, corresponding to a charge $Z=1$ and asymptotic momentum $\boldsymbol{k}_b$. In Eq. (10) $M_{jk_b}=\langle\psi_j|\boldsymbol{\mathcal{E}}_0\cdot\boldsymbol{R}|\psi_{k_b}^{(-)}\rangle$ is a dipole coupling matrix element.

In both Eqs. (7) and (10), the field-free excited states of helium (both discrete and continuous) have been taken to be of the form

$$\psi_j(\boldsymbol{r}_1,\boldsymbol{r}_2)=\frac{1}{\sqrt{2}}[\phi_{1s}(Z=2,\boldsymbol{r}_1)\phi_{n\ell m}(Z=1,\boldsymbol{r}_2)+\phi_{1s}(Z=2,\boldsymbol{r}_2)\phi_{n\ell m}(Z=1,\boldsymbol{r}_1)], \tag{14}$$

where $\phi_{n\ell m}(Z,\boldsymbol{r})$ is a hydrogenic wave function corresponding to the $n\ell m$ state, and n can take both discrete and continuous values. We also note that $\phi_{1s}(Z=2,\boldsymbol{r})=\phi_0^{\mathrm{He}^+}(\boldsymbol{r})$. The energies E_j corresponding to the wave functions ψ_j of Eq. (14) are given by $E_j=E_0^{\mathrm{He}^+}+E_n^{Z=1}$, where $E_n^{Z=1}$ are the hydrogen atom energies (both discrete and continuous). In writing Eq. (14), we have neglected the contribution of doubly excited target states, which is known to be small for excitation processes.

Equation (4) is evaluated analytically to obtain the first Born ionization S-matrix element, which for the present laser-assisted $(e,2e)$ reaction is given by

$$S_{\mathrm{ion}}^{B_1}=i(2\pi)^{-1}\sum_{\ell=-\infty}^{\ell=+\infty}\delta\left(E_{k_a}+E_{k_b}+E_0^{\mathrm{He}^+}-E_{k_i}-E_0^{\mathrm{He}}-\ell\omega\right)f_{\mathrm{ion}}^{B_1,\ell}. \tag{15}$$

Here $f_{\mathrm{ion}}^{B_1,\ell}$ is the first Born amplitude for the laser-assisted $(e,2e)$ process involving the exchange of ℓ photons. This quantity is given by

$$f_{\mathrm{ion}}^{B_1,\ell}=f_1+f_2+f_3, \tag{16}$$

with

$$f_1=-2\Delta^{-2}\left\langle\psi_{k_b}^{(-)}\middle|e^{i\boldsymbol{\Delta}\cdot\mathbf{r}_1}+e^{i\boldsymbol{\Delta}\cdot\mathbf{r}_2}|\psi_0\right\rangle J_\ell(\lambda), \tag{17a}$$

$$f_2=i\Delta^{-2}\sum_j\left\langle\psi_{k_b}^{(-)}\middle|e^{i\boldsymbol{\Delta}\cdot\mathbf{r}_1}+e^{i\boldsymbol{\Delta}\cdot\mathbf{r}_2}|\psi_j\right\rangle M_{j0}\times\left(\frac{J_{\ell-l}(\lambda)}{E_j-E_0^{\mathrm{He}}-\omega}-\frac{J_{\ell+l}(\lambda)}{E_j-E_0^{\mathrm{He}}+\omega}\right), \tag{17b}$$

and

$$f_3=i\Delta^{-2}\sum_j\langle\psi_j|e^{i\boldsymbol{\Delta}\cdot\mathbf{r}_1}+e^{i\boldsymbol{\Delta}\cdot\mathbf{r}_2}|\psi_0\rangle M_{jk_b}^*\times\left(\frac{J_{\ell-l}(\lambda)}{E_j-E_{k_b}-E_0^{\mathrm{He}^+}+\omega}-\frac{J_{\ell+l}(\lambda)}{E_j-E_{k_b}-E_0^{\mathrm{He}^+}-\omega}\right)-2\Delta^{-2}\boldsymbol{k}_b\cdot\boldsymbol{\alpha}_0J_\ell'(\lambda)\left\langle\psi_{k_b}^{(-)}\middle|e^{i\boldsymbol{\Delta}\cdot\mathbf{r}_1}+e^{i\boldsymbol{\Delta}\cdot\mathbf{r}_2}|\psi_0\right\rangle. \tag{17c}$$

In these equations, J_ℓ is a Bessel function of order ℓ, $\boldsymbol{\Delta}=\boldsymbol{k}_i-\boldsymbol{k}_a$ is the momentum transfer, and $\lambda=(\boldsymbol{\Delta}-\boldsymbol{k}_b)\cdot\boldsymbol{\alpha}_0$.

Let us now consider exchange effects in laser-assisted $(e,2e)$ collisions. The exchange amplitude with the transfer of ℓ photons is approximated by its dominant part coming from the first Born approximation

$$g_{\mathrm{ion}}^{\ell}(\boldsymbol{\Delta})\simeq J_\ell(\lambda)g_{\mathrm{ion}}^{\mathrm{Och}}, \tag{18}$$

with

$$g_{\mathrm{ion}}^{\mathrm{Och}}=\frac{\Delta^2}{k_i^2}f_{\mathrm{ion}}^{B_1}. \tag{19}$$

where $g_{\mathrm{ion}}^{\mathrm{Och}}$ is the exchange amplitude in the Ochkur approximation [47], and $f_{\mathrm{ion}}^{B_1}$ is the field-free first Born ionization amplitude. The term proportional to k_i^{-3} [48] was not taken into account in our calculation since the term proportional to k_i^{-2} is the leading term in the exchange scattering amplitude.

The first Born triple differential cross section corresponding to the $(e,2e)$ process accompanied by the transfer of ℓ photons is then given by

$$\frac{d^3\sigma_{\mathrm{ion}}^{B_1,\ell}}{d\Omega_a d\Omega_b dE}=\frac{k_ak_b}{k_i}\left|f_{\mathrm{ion}}^{B_1,\ell}-g_{\mathrm{ion}}^{\ell}\right|^2. \tag{20}$$

The second Born S-matrix element is much more complicated than the first Born one discussed above. It is given by the expression

$$S_{\mathrm{ion}}^{B_2}=-i\int_{-\infty}^{+\infty}dt\int_{-\infty}^{+\infty}dt'\left\langle\chi_{k_a}(\boldsymbol{r}_0,t)\phi_{k_b}(\boldsymbol{X},t)\middle|V_d(\boldsymbol{r}_0,\boldsymbol{X})\times G_0^{(+)}(\boldsymbol{r}_0,\boldsymbol{X},t,\boldsymbol{r}_0',\boldsymbol{X}',t')V_d(\boldsymbol{r}_0',\boldsymbol{X}')\times\left|\chi_{k_i}(\boldsymbol{r}_0',t')\phi_0(\boldsymbol{X}',t')\right\rangle, \tag{21}$$

where $G_0^{(+)}$ is the causal propagator. This term is second order in the electron-atom interaction potential V_d and contains atomic wave functions corrected to first order in $\mathcal{E}_0$ for the target dressed states. One finds that $S_{\mathrm{ion}}^{B_2}$ is the sum of two terms which are respectively of zero and first order in $\mathcal{E}_0$. We may concentrate our discussion on the computation of the zero-order term $S_{\mathrm{ion}}^{B_2,0}$.

Thus, the lowest-order component $S_{\mathrm{ion}}^{B_2,0}$ evaluated at the shifted momenta $\boldsymbol{\Delta}_i$ and $\boldsymbol{\Delta}_f$ can be expressed in terms of a second Born amplitude as

$$S_{\mathrm{ion}}^{B_2,0}=-(2\pi)^{-1}i\sum_{\ell=-\infty}^{\ell=+\infty}\delta\left(E_{k_a}+E_{k_b}+E_0^{\mathrm{He}^+}-E_{k_i}-E_0^{\mathrm{He}}-\ell\omega\right)f_{\mathrm{ion}}^{B_2,\ell,0}(\boldsymbol{\Delta}), \tag{22}$$

where

$$f_{\mathrm{ion}}^{B_2,\ell,0}(\boldsymbol{\Delta})=J_\ell(\lambda)f_{\mathrm{ion}}^{B_2}(\boldsymbol{\Delta}), \tag{23}$$

with

$$f_{\rm ion}^{B_2}(\mathbf{\Delta}) = -\frac{1}{\pi^2}\int_0^{+\infty} d\boldsymbol{q} \times \frac{\langle \psi_{k_b}^{(-)} \mid \widetilde{V}_d(\mathbf{\Delta}_f, \boldsymbol{X}) G_c(\xi') \widetilde{V}_d(\mathbf{\Delta}_i, \boldsymbol{X}) \mid \psi_0 \rangle}{\Delta_i^2 \Delta_f^2}, \quad (24)$$

where $\mathbf{\Delta}_i = \boldsymbol{k}_i - \boldsymbol{q}$, $\mathbf{\Delta}_f = \boldsymbol{q} - \boldsymbol{k}_a$, and $\mathbf{\Delta} = \mathbf{\Delta}_i + \mathbf{\Delta}_f$. $\widetilde{V}_d(\mathbf{\Delta},\mathbf{X}) = e^{i\mathbf{\Delta}\cdot\mathbf{r}_1} + e^{i\mathbf{\Delta}\cdot\mathbf{r}_2} - 2$ and $G_c(\xi') = \sum_n \frac{|\psi_n\rangle\langle\psi_n|}{\xi' - E_n}$ is the Coulomb Green's function with argument $\xi' = E_{k_i} + E_0^{\rm He} - E_q - E_{k_b} + \ell\omega$, where E_q is the virtual projectile energy.

The electron-atom amplitude with the transfer of ℓ photons may be written in the second Born approximation as

$$f_{\rm ion}^{\ell}(\mathbf{\Delta}) = f_{\rm ion}^{B_1,\ell}(\mathbf{\Delta}) + f_{\rm ion}^{B_2,\ell,0}(\mathbf{\Delta}). \quad (25)$$

The integral in Eq. (24) over the virtual projectile states $\chi_q(\mathbf{r}_0,t)$, with wave vector $\boldsymbol{q}$, is prohibitively difficult, and is actually zero at some values of incident electron energies. We overcome this difficulty by using the exact upper boundary of integral (24) over the virtual projectile, which is obtained by the requirement [49]

$$q \leqslant \inf(k_i, k_a). \quad (26)$$

The first and second Born amplitudes for the laser-assisted electron-impact ionization have been computed by expanding the atomic wave functions onto a Sturmian basis [26,50]. This method of calculation constitutes an important advantage with respect to earlier computations relying on the closure approximation [37,45,51–53].

The expression of the triple differential cross section in the second Born approximation accompanied by the transfer of ℓ photons is given by

$$\frac{d^3\sigma_{\rm ion}^{B_2,\ell}}{d\Omega_a\, d\Omega_b\, dE} = \frac{k_a k_b}{k_i}\left| f_{\rm ion}^{\ell} - g_{\rm ion}^{\ell} \right|^2. \quad (27)$$

III. RESULTS AND DISCUSSION

In this section, we report on the results of a study into the laser-assisted $(e, 2e)$ reaction of a helium target for which the prospects of performing experiments are favorable. The fully differential cross sections are calculated in the coplanar asymmetric geometry. Without loss of generality, we choose the origin of the coordinate system to be the target nucleus and the wave vector of the incoming electron along the z axis. We set the x axis in the plane defined by the incident momentum and the polarization vector of the laser field. The angle of the scattered electron and that of the ejected electron are denoted respectively by θ_a and θ_b; θ_a is measured in the counterclockwise direction, while θ_b is measured in the clockwise direction. The azimuth angle between the scattering plane and the zx plane is referred to by ϕ. Our detailed calculations are evaluated for two distinct orientations in which the laser polarization vector $\hat{\varepsilon}$ is either parallel or perpendicular to the momentum transfer $\mathbf{\Delta}$ (see Fig. 1). We present our results for the following parameters: the incident electron energy is $E_{k_i} = 40$ eV, the ejected electron energy is $E_{k_b} = 5$ eV, and the laser photon energy is $\omega = 1.17$ eV, which is of interest because it corresponds to the first harmonic of a Nd:YAG laser. The electric field amplitude is $\mathcal{E}_0 = 1 \times 10^7$ V/cm,

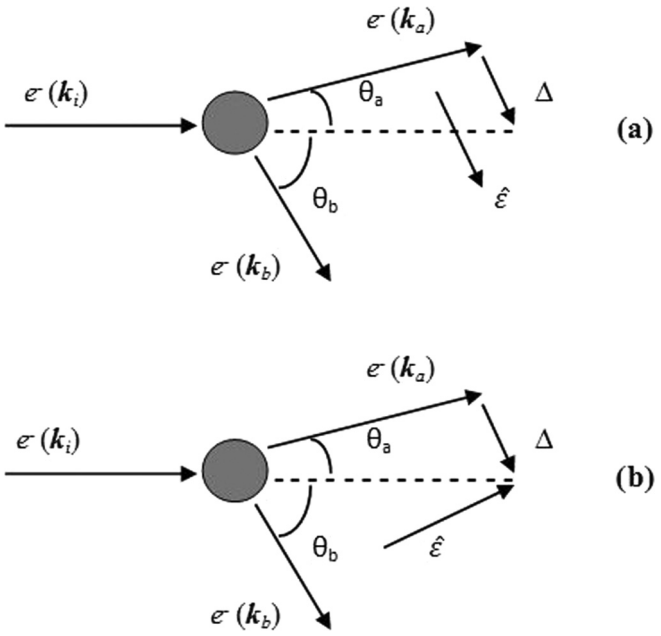

FIG. 1. Selected orientations of laser polarization for electron-impact ionization in the presence of a linearly polarized laser field: (a) $\hat{\varepsilon} \parallel \mathbf{\Delta}$ and (b) $\hat{\varepsilon} \perp \mathbf{\Delta}$.

the scattering angle is $\theta_a = 4^\circ$, and the azimuth angle is $\phi = 0^\circ$. For this choice, higher-order contributions such as a second-order Born term and exchange corrections become important and are discussed below.

In what follows, the detection energy of the ejected electron is kept fixed at 5 eV. Accordingly, when the projectile-target system exchanges photons with the laser field, the final energy of the scattered electron changes as given by the energy conservation equation (3), which here reads

$$E_{k_a} = E_{k_i} + E_0^{\rm He} - E_0^{\rm He^+} - E_{k_b} + \ell\omega. \quad (28)$$

We have chosen first to address the case of laser-assisted electron-impact ionization in the course of which no photons are exchanged between the projectile-atom system and the laser field; i.e., we consider the case in which the energy of the scattered electron is the same as the one for the field-free case. This corresponds to replacing ℓ by 0 in the energy conservation relation. It then makes sense to compare the TDCSs for field-free and laser-assisted collisions, computed within the first and second Born approximations.

In Fig. 2, we show the variations of the TDCSs for no photon transfer. In the field-free situation, the results revealed the presence of two different peaks: the binary and the recoil peaks. The binary peak is the result of an encounter between the incoming electron and one of the atomic electrons and is essentially independent of the nucleus. In this case the scattered and ejected electrons emerge on opposite sides of the incident electron direction. The recoil peak is governed by the attraction between the electron and the nucleus. In fact, the electron which has been initially scattered in the direction of the binary peak has subsequently suffered a reflection due to the attractive potential of the ion. We observe that, in a second Born treatment of the field-free $(e, 2e)$ collisions, the angular distribution of the ejected electron admits the

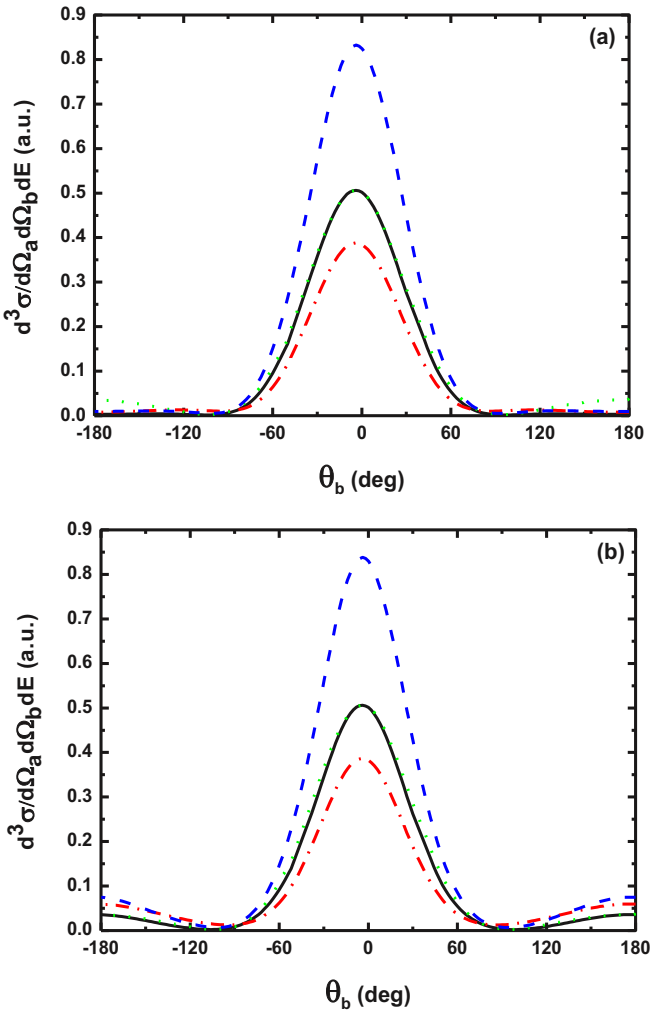

FIG. 2. (Color online) Triple differential cross sections corresponding to the laser-assisted electron-impact ionization process of a helium atom as a function of the ejected angle θ_b with no net exchange of photons ($\ell = 0$). The laser frequency is 1.17 eV and the electric field strength is 1×10^7 V/cm. The incident electron energy is $E_{k_i} = 40$ eV, the ejected electron energy is $E_{k_b} = 5$ eV, and the scattering angle is $\theta_a = 4^\circ$. The laser polarization in (a) is parallel to the momentum transfer ($\hat{\varepsilon} \parallel \mathbf{\Delta}$) and in (b) perpendicular to the momentum transfer ($\hat{\varepsilon} \perp \mathbf{\Delta}$). Solid lines, second Born approximation results with including exchange effects; dashed lines, second Born approximation results without including exchange effects; dash-dotted lines, first Born approximation results; dotted lines, field-free results in the second Born approximation.

direction of the momentum transfer $\mathbf{\Delta}$ as a symmetry axis. Indeed, the TDCSs in Fig. 2 are symmetrical with respect to the angles $\theta_b = 4^\circ$ and $180^\circ - \theta_b$, which correspond to the maxima of the binary and recoil peaks, respectively. The second Born TDCS including exchange effects deviates from the field-free one in the vicinity of the recoil peak when $\hat{\varepsilon} \parallel \mathbf{\Delta}$ while the two results are almost similar when $\hat{\varepsilon} \perp \mathbf{\Delta}$ as long as the laser field strength is not larger than $\sim 5 \times 10^7$ V/cm. When $\hat{\varepsilon} \parallel \mathbf{\Delta}$, the recoil peak almost disappears in the first and second Born approximations with respect to the field-free case. This indicates that, for this laser polarization direction, the ejected electron is weakly attracted by the residual nucleus. For both parallel- and perpendicular-field vectors, the binary peak is dominant in the results of $\ell = 0$ which means that the electron-electron interaction is important against the attraction between the electron and the nucleus. Comparing with the first-order Born results, the binary peak is greatly enhanced in the second Born approximation, whereas the recoil peak is slightly suppressed.

We now turn to the examination of the importance of exchange effects in laser-assisted single ionization of a helium atom by slow electrons. It is well known from field-free electron-atom collision theory that exchange effects lose their importance when the velocity of the incoming electron is considerably larger than that of the atomic electrons [54]. In order to demonstrate the importance of exchange effects, we have chosen to compare the corresponding second-order Born TDCSs results by including the exchange amplitude with the TDCSs generated singly by the direct amplitude. It can be seen from Fig. 2 that the inclusion of the exchange alters the magnitude of the TDCS by lowering it significantly in comparison to that of the SBA without exchange; i.e., the TDCSs are mainly contributed by the exchange amplitude which shows that the exchange effects between two outgoing electrons cannot be ignored. This effect is manifested more clearly for an atomic system with more than one electron [55] and for slow velocities of the incident electron [54].

Figure 3 shows our results of triple differential cross sections when the ionizing process is accompanied by the absorption of one photon ($\ell = 1$). We observe that, for both laser polarization directions, the second Born approximation gives an enhanced binary peak and a reduced recoil peak in contrast to the results of the FBA. In Fig. 3(a), we notice a dominance of the recoil peak with a notable reduction of the magnitude of the binary peak. This can be interpreted in the following way: the binary peak results from the direct interaction between the projectile and the atomic electron. In such an electron-electron encounter, the probability for exchanging a photon with the field is very small. This is the same situation as for the bremsstrahlung radiation emitted in electron-electron collisions. In contrast, the recoil peak results from a strong interaction with the nucleus, and the probability for undergoing a radiative transition is much higher. Again, this situation is similar to what is observed when discussing bremsstrahlung spectra in atoms. This may explain why the recoil peak becomes larger than the binary one. In Fig. 3(a) only the binary peak is split, whereas in Fig. 3(b) both the binary and recoil peaks are split. The splitting of the peaks is a typical signature of the laser effects on the TDCSs. In fact, the presence of the laser breaks the symmetry of the angular distribution which, without the field, is symmetrical with respect to the orientation of $\mathbf{\Delta}$. This is due to the presence of a new preferred direction associated with the laser field polarization. This behavior is owing to the fact that the argument of the Bessel functions $J_\ell(\lambda)$, appearing in the direct amplitudes of Eqs. (17) and (23), varies with the angle θ_b leading thus to the observed zeros of the Bessel functions which coincide with the minimums of the TDCSs. Note that, for $\hat{\varepsilon} \parallel \mathbf{\Delta}$ and $\hat{\varepsilon} \perp \mathbf{\Delta}$, the effects of exchange are to reduce the magnitudes of the cross sections. This indicates the importance of including exchange in calculating ionization cross sections

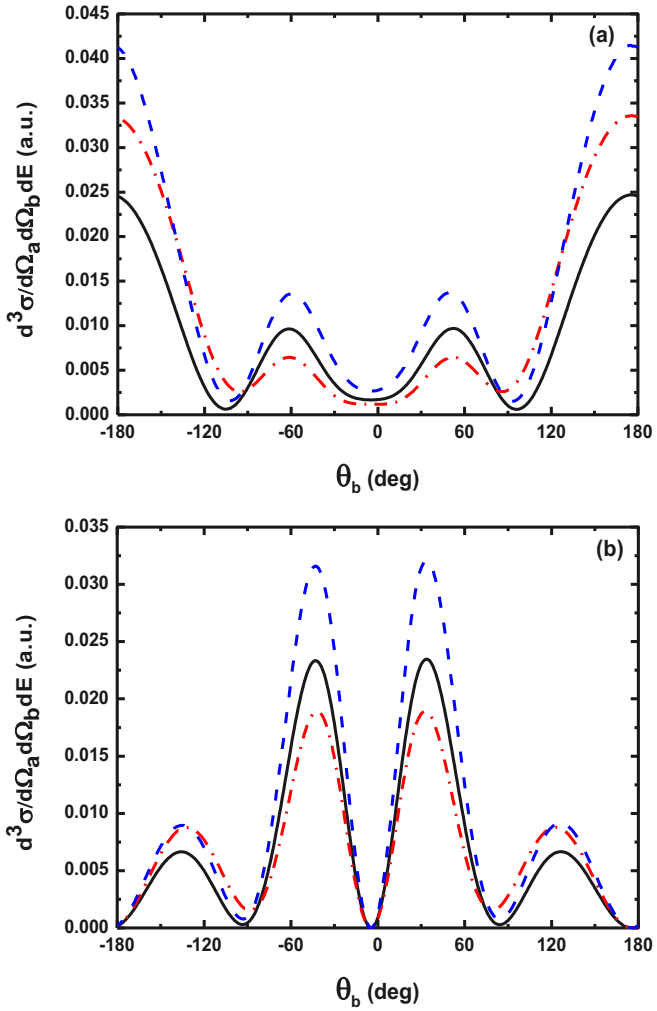

FIG. 3. (Color online) All the parameters are the same as in Fig. 2, but with the absorption of one photon ($\ell = 1$).

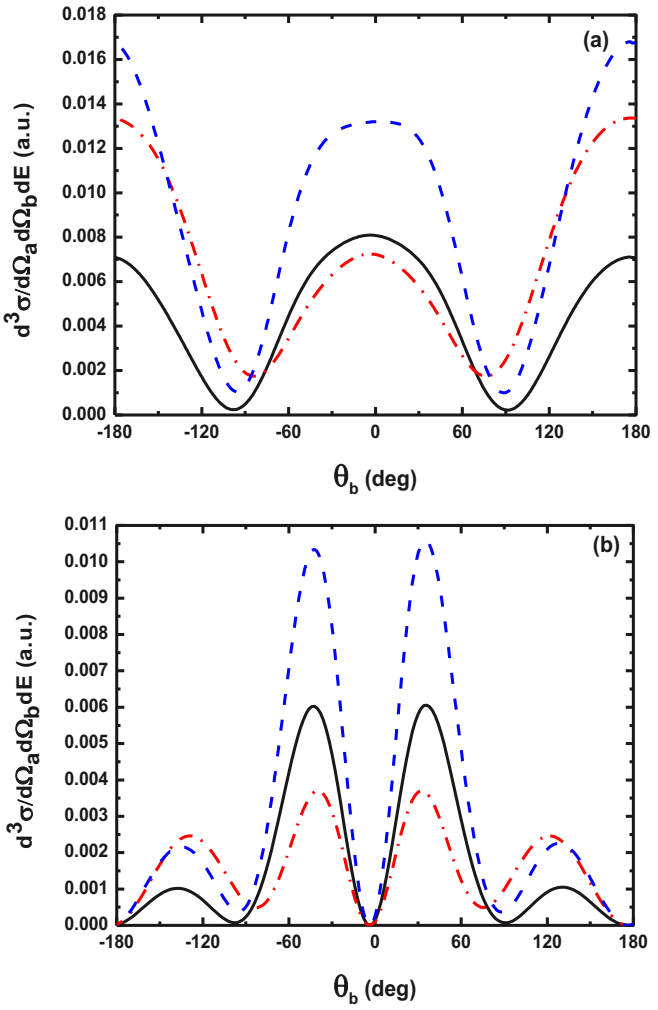

FIG. 4. (Color online) All the parameters are the same as in Fig. 2, but with the emission of one photon ($\ell = -1$).

for a helium target at low-incident-energy range. Changing the polarization orientation significantly affects the angular distribution. Indeed, in Figs. 3(a) and 3(b), $\mathbf{\Delta} - \boldsymbol{k}_b$ is the same; however, the quantity $\boldsymbol{\alpha}_0 \cdot (\mathbf{\Delta} - \boldsymbol{k}_b)$ is different since the orientation of $\boldsymbol{\alpha}_0$ is different.

In Fig. 4, the dependence of the cross sections on the ejected electron angle is shown for the emission of one photon ($\ell = -1$). When the laser polarization vector is parallel to the momentum transfer, the splitting of the binary and recoil peaks disappears due to the absence of a new preferred direction, responsible for the splitting, associated with the laser field. In this case, the symmetry with respect to the momentum transfer $\mathbf{\Delta}$ is restored. The second-order Born model reproduces higher triple differential cross sections in the binary peak, whereas it yields lower cross sections in the recoil peak than the first Born treatment does. When $\hat{\varepsilon} \parallel \mathbf{\Delta}$, the binary and recoil collision become equally important in the SBA. Another interesting point is the fact that the angular distribution is strongly modified as the respective magnitudes of the binary and recoil peaks are reversed. Indeed, the recoil (binary) peak for $\hat{\varepsilon} \parallel \mathbf{\Delta}$ ($\hat{\varepsilon} \perp \mathbf{\Delta}$) becomes dominant over the binary (recoil) peak. The observed inversion between the magnitudes of the binary and recoil peaks is likely to result from the physical mechanism leading to the occurrence of each of those peaks. This clearly shows that the collision dynamics is strongly affected by the orientation of the laser polarization, even at moderate laser intensities. By comparing Figs. 3(a) and 4(a) and Figs. 3(b) and 4(b), we observe that the inverse bremsstrahlung processes dominate those of stimulated bremsstrahlung, meaning that the system absorbs net energy from the radiation background.

The differences observed in TDCSs between Figs. 3(a) and 3(b) and between Figs. 4(a) and 4(b) are strongly dependent on the orientation of the laser polarization. In fact, the first and second Born amplitudes of Eqs. (17) and (23) depend on the laser polarization direction via the argument λ of the Bessel functions, i.e., via the scalar products $\boldsymbol{\alpha}_0 \cdot \mathbf{\Delta}$ and $\boldsymbol{\alpha}_0 \cdot \boldsymbol{k}_b$. In a more physical perspective, the scalar product $\boldsymbol{\alpha}_0 \cdot \mathbf{\Delta}$ can be associated to the coupling of the laser field with the scattered electron which experiences the momentum change $\mathbf{\Delta}$ during the course of the collision, while the scalar product $\boldsymbol{\alpha}_0 \cdot \boldsymbol{k}_b$ corresponds to the coupling of the laser field with the ejected electron. Changing the orientation of $\hat{\varepsilon}$ with respect to these characteristic momenta allows one to modify accordingly the coupling of the field with either of the

electrons. The magnitude of the cross sections for $\hat{\varepsilon} \parallel \mathbf{\Delta}$ is larger than that for $\hat{\varepsilon} \perp \mathbf{\Delta}$. Indeed, the choice $\hat{\varepsilon} \parallel \mathbf{\Delta}$ allows us to maximize the cross sections since the argument of the Bessel functions appearing in Eqs. (17) and (23) is also maximized. This is due to the fact that the coupling between the laser and the scattered electron reaches the maximum in this laser orientation.

IV. CONCLUSION

In this work, we have performed a study of laser-assisted electron-impact ionization of a helium atom at an incident energy of 40 eV. The motivation was to extend our previous studies in hydrogen to the case of helium, which is expected to be more accessible to experiments. We report accurate results of triple differential cross sections using a second-order Born treatment. In addition, the exchange effects have been considered. Numerical results show that the TDCSs are notably modified by taking into account exchange effects. Important modifications of the angular distribution of the ejected electron can take place by changing the orientation of the laser polarization. Furthermore, second-order Born calculations are significantly different from the results obtained in the first-order Born theory. When we add the contribution of the second Born term we observe a fall of the recoil lobe amplitude and a rise of the binary lobe amplitude for both $\hat{\varepsilon} \parallel \mathbf{\Delta}$ and $\hat{\varepsilon} \perp \mathbf{\Delta}$ orientations.

[1] L. G. Christophorou and J. K. Olthoff, *Fundamental Electron Interactions with Plasma Processing Gases* (Kluwer Academic, New York, 2004).

[2] L. Campbell and M. J. Brunger, Plasma Sources Sci. Technol. **22**, 013002 (2013).

[3] B. Boudaiffa, P. Cloutier, D. Hunting, M. A. Huels, and L. Sanche, Science **287**, 1658 (2000).

[4] H. Ehrhardt, M. Schulz, T. Tekaat, and K. Willmann, Phys. Rev. Lett. **22**, 89 (1969).

[5] J. Röder, H. Ehrhardt, C. Pan, A. F. Starace, I. Bray, and D. V. Fursa, Phys. Rev. Lett. **79**, 1666 (1997).

[6] J. Röder, M. Baertschy, and I. Bray, Phys. Rev. A **67**, 010702(R) (2003).

[7] J. G. Childers, K. E. James, M. Hughes, I. Bray, M. Baertschy, and M. A. Khakoo, Phys. Rev. A **68**, 030702(R) (2003).

[8] M. Dürr, C. Dimopoulou, A. Dorn, B. Najjari, I. Bray, D. V. Fursa, Z. Chen, D. H. Madison, K. Bartschat, and J. Ullrich, J. Phys. B **39**, 4097 (2006).

[9] X. Ren, A. Senftleben, T. Pflüger, A. Dorn, J. Colgan, M. S. Pindzola, O. Al-Hagan, D. H. Madison, I. Bray, D. V. Fursa, and J. Ullrich, Phys. Rev. A **82**, 032712 (2010).

[10] X. Ren, I. Bray, D. V. Fursa, J. Colgan, M. S. Pindzola, T. Pflüger, A. Senftleben, S. Xu, A. Dorn, and J. Ullrich, Phys. Rev. A **83**, 052711 (2011).

[11] C. Pan and A. F. Starace, Phys. Rev. Lett. **67**, 185 (1991).

[12] C. T. Whelan, R. J. Allan, J. Rasch, H. R. J. Walters, X. Zhang, J. Roder, K. Jung, and H. Ehrhardt, Phys. Rev. A **50**, 4394 (1994).

[13] D. H. Madison, R. V. Calhoun, and W. N. Shelton, Phys. Rev. A **16**, 552 (1977).

[14] G. Purohit, R. Choubisa, V. Patidar, and K. K. Sud, Phys. Scr. **69**, 208 (2004).

[15] I. Bray, Phys. Rev. Lett. **89**, 273201 (2002).

[16] M. Brauner, J. S. Briggs, and H. Klar, J. Phys. B **22**, 2265 (1989).

[17] I. Bray, D. V. Fursa, J. Roder, and H. Ehrhardt, Phys. Rev. A **57**, R3161(R) (1998).

[18] J. Colgan, M. S. Pindzola, G. Childers, and M. A. Khakoo, Phys. Rev. A **73**, 042710 (2006).

[19] A. T. Stelbovics, I. Bray, D. V. Fursa, and K. Bartschat, Phys. Rev. A **71**, 052716 (2005).

[20] Y. Wang, L. Jiao, and Y. Zhou, Phys. Lett. A **376**, 2122 (2012).

[21] P. Cavaliere, G. Ferrante, and C. Leone, J. Phys. B **13**, 4495 (1980).

[22] J. Banerji and M. H. Mittleman, J. Phys. B **14**, 3717 (1981).

[23] R. Zangara, P. Cavaliere, C. Leone, and G. Ferrante, J. Phys. B **15**, 3881 (1982).

[24] C. J. Joachain, P. Francken, A. Maquet, P. Martin, and V. Véniard, Phys. Rev. Lett. **61**, 165 (1988).

[25] D. Khalil, A. Maquet, R. Taïeb, C. J. Joachain, and A. Makhoute, Phys. Rev. A **56**, 4918 (1997).

[26] G. Duchateau, E. Cormier, and R. Gayet, Phys. Rev. A **66**, 023412 (2002).

[27] S. M. Li, J. Chen, and Z. F. Zhou, J. Phys. B **35**, 557 (2002).

[28] A. Chattopadhyay and C. Sinha, Phys. Rev. A **72**, 053406 (2005).

[29] S. M. Li, J. Berakdar, S. T. Zhang, and J. Chen, J. Electron Spectrosc. Relat. Phenom. **161**, 188 (2007).

[30] C. Höhr, A. Dorn, B. Najjari, D. Fischer, C. D. Schröter, and J. Ullrich, Phys. Rev. Lett. **94**, 153201 (2005).

[31] F. W. Byron, Jr., C. J. Joachain, and B. Piraux, J. Phys. B **13**, L673 (1980).

[32] A. Pathak and M. K. J. Srivastava, J. Phys. B **14**, L773 (1981).

[33] E. Weigold, C. J. Noble, S. T. Hood, and I. Fuss, J. Phys. B **12**, 291 (1979).

[34] H. Ehrhardt, M. Fischer, and K. Jung, Z. Phys. A **304**, 119 (1982).

[35] F. W. Byron, Jr., C. J. Joachain, and B. Piraux, J. Phys. B **15**, L293 (1982).

[36] F. W. Byron, Jr., C. J. Joachain, and B. Piraux, J. Phys. B **18**, 3203 (1985).

[37] M. Y. Zheng and S. M. Li, Phys. Rev. A **82**, 023414 (2010).

[38] M. Y. Zheng, G. Qin, and S. M. Li, Phys. Rev. A **82**, 033425 (2010).

[39] C. J. Joachain, A. Makhoute, A. Maquet, and R. Taïeb, Z. Phys. D **23**, 397 (1992).

[40] A. Makhoute, D. Khalil, A. Maquet, C. J. Joachain, and R. Taïeb, J. Phys. B **32**, 3255 (1999).

[41] S. M. Li, J. Berakdar, S. T. Zhang, and J. Chen, J. Phys. B **38**, 1291 (2005).

[42] C. Dal Cappello, A. Haddadou, F. Menas, and A. C. Roy, J. Phys. B **44**, 015204 (2011).

[43] A. Makhoute, I. Ajana, and D. Khalil, Phys. Rev. A **90**, 053415 (2014).

[44] D. M. Volkov, Z. Phys. **94**, 250 (1935).

[45] F. W. Byron, Jr., P. Francken, and C. J. Joachain, J. Phys. B **20**, 5487 (1987).
[46] F. W. Byron, Jr. and C. J. Joachain, Phys. Rev. **146**, 1 (1966).
[47] V. I. Ochkur, Sov. Phys.–JETP **18**, 503 (1964).
[48] L. A. Burkova and V. I. Ochkur, Sov. Phys.–JETP **49**, 38 (1979).
[49] M. Bouzidi, A. Makhoute, D. Khalil, A. Maquet, and C. J. Joachain, J. Phys. B **34**, 737 (2001).
[50] R. Taïeb, V. Véniard, A. Maquet, S. Vucic, and R. M. Potvliege, J. Phys. B **24**, 3229 (1991).
[51] F. W. Byron, Jr. and C. J. Joachain, J. Phys. B **17**, L295 (1984).
[52] P. Francken and C. J. Joachain, Phys. Rev. A **35**, 1590 (1987).
[53] P. Francken, Y. Attaourti, and C. J. Joachain, Phys. Rev. A **38**, 1785 (1988).
[54] G. Ferrante, C. Leone, and F. Trombetta, J. Phys. B **15**, L475 (1982).
[55] I. Ajana, A. Makhoute, D. Khalil, and A. Dubois, J. Phys. B **47**, 175001 (2014).